Commun. Optim. Theory 2026 (2026) 5 https://doi.org/10.23952/cot.2026.5

MATHRES Communications in Optimization Theory
Available online at http://cot.mathres.org

TWO-DIMENSIONAL REACHABLE SET FOR DUBINS CAR UNDER AN INTEGRAL CONSTRAINT ON CONTROL

VALERII PATSKO[1,*], GEORGII TRUBNIKOV[2], ANDREY FEDOTOV[1]

[1]Krasovskii Institute of Mathematics and Mechanics, Ekaterinburg, Russia
[2]Ural Federal University named after the first President of Russia B. N. Yeltsin, Ekaterinburg, Russia

Dedicated to Professor F.L. Chernousko on the occasion of his 87th birthday

Abstract. The kinematic model "Dubins car" is considered. A scalar control is constrained by a quadratic integral constraint. A three-dimensional initial phase state is fixed, and a two-dimensional reachable set is constructed "at the instant" on the plane of geometric coordinates. The analysis is based on the Pontryagin maximum principle. Examples of numerical construction of the reachable set are given. A comparison is made with the case of a geometric control constraint.

Keywords. Dubins car; Integral control constraint, Two-dimensional reachable set in geometric coordinates, Pontryagin maximum principle, Numerical construction.

2020 Mathematics Subject Classification. 33E05, 49K15, 49M05, 93B03, 93C10.

1. INTRODUCTION

"Dubins car" is one of the most popular nonlinear kinematic models of a controlled object motion on a plane. Another name is "unicycle". Variables x, y define a point position of the object, an angle φ characterizes a direction of the velocity vector. The speed value is considered constant. It is usually assumed to be equal to 1. A scalar control $u(t)$ determines the instantaneous angular velocity of the object: $\dot{\varphi} = u(t)$. The *geometric* constraint $|u(t)| \le \mu$ on control is typical. Such a model with the geometric control constraint is widely used in simplified consideration of an aircraft motion in a horizontal plane, in solving various problems of controlled motion of ships, underwater vehicles, etc. Of recent works, we note, for example, [1, 2].

In many cases, it is natural to consider a given three-dimensional initial phase state $(x(t_0), y(t_0), \varphi(t_0))^{\mathsf{T}}$ and to investigate (for $t \ge t_0$) the motions in the coordinates x, y. For example, with the help of which open-loop control $u(\cdot)$ can the object be transferred in the least amount of time to a

*Corresponding author.
E-mail address: patsko@imm.uran.ru (V. Patsko), jora_it@mail.ru (G. Trubnikov), andreyfedotov@mail.ru (A. Fedotov).

Received August 31, 2024; Accepted January 25, 2025.

given geometric position $(x^*, y^*)^\mathsf{T}$? To solve similar problems, the notion of *a two-dimensional reachable set* $\mathcal{G}(t_f, \mu)$ is useful: the set of all points $(x, y)^\mathsf{T}$, to each of which it is possible to transfer the object at the time t_f from the fixed initial three-dimensional phase state. Description of properties of the set $\mathcal{G}(t_f, \mu)$, including an investigation of controls leading to its boundary, constituted "folklore" in the literature on mathematical control theory in the 70s years of the last century (see, for example, [3]). The set $\mathcal{G}(t_f, \mu)$ for the case of the geometric control constraint is most fully described in [4].

In this work, we study the reachable set $\mathcal{G}(t_f, \mu)$ under an *integral* quadratic constraint

$$\int_{t_0}^{t_f} u^2(t)dt \le \mu. \tag{1.1}$$

There is no restriction on instantaneous values $u(t)$. Consideration of the integral constraint is very important because it relates to the "energy" expended in turns.

Problems with the same kinematics as in the Dubins car, but with optimization of the integral functional

$$J(u(\cdot)) = \int_{t_0}^{t_f} u^2(t)dt, \tag{1.2}$$

were studied back at the end of the 17th century. In particular, such a problem was investigated in detail in the book [5, Appendix 1] by L. Euler published in 1744. Later, the notion "Euler elastica" arose. This notion began to be used to denote motions that satisfy the necessary optimality conditions under given three-dimensional edge conditions $(x(t_0), y(t_0), \varphi(t_0))^\mathsf{T}$ and $\big(x(t_f), y(t_f), \varphi(t_f)\big)^\mathsf{T}$. The history of works related to the Euler elasticae is well described, for example, in [6].

The works of Sachkov and Ardentov were devoted (see, for example, [7, 8]) to issues of local and global optimality of the Euler elasticae when the right edge condition is three-dimensional. If the right edge condition is two-dimensional and specified in coordinates x, y, then such elasticae are called free [9]. Optimization problems of the Bolza quadratic cost functional for systems with the Dubins car kinematics are also investigated [10].

Studying the two-dimensional reachable set $\mathcal{G}(t_f, \mu)$, we use in this work the facts established under the integral constraint for the three-dimensional reachable set $G(t_f, \mu)$. Corresponding statements based on the Pontryagin maximum principle (PMP) with a clarification from work [11] for the motions, leading to the boundary of the set $G(t_f, \mu)$, are given in [12, 13].

Paper [14] substantiates an additional edge condition for the adjoint PMP system, which is satisfied by motions leading to the boundary of the two-dimensional set $\mathcal{G}(t_f, \mu)$. Based on it, we prove the statement that any open-loop control $u(\cdot)$ leading to the boundary of the set $\mathcal{G}(t_f, \mu)$ is continuous and has at most one instant of change of control sign. This allows us to numerically construct the boundary of the reachable set $\mathcal{G}(t_f, \mu)$. The structural properties of the boundary are in many ways similar to what occurs for the set $\mathcal{G}(t_f, \mu)$ under a geometric control constraint. But there is no complete analogy, and constructing the boundary of the reachable set under the integral constraint is more difficult than with the geometric constraint.

The presentation in the paper is carried out according to the following scheme. After Section 2 on the formulation of the problem, Section 3 comes with a description of symmetry properties of the three-dimensional reachable set with an indication of how they are transformed for the case of the two-dimensional set. Such properties are a consequence of the specific kinematics of the Dubins car and can be proven without using the PMP. Then, in Section 3, we derive

basic relations of the PMP with respect to the three-dimensional set $G(t_f,\mu)$ and formulate a theorem on six types of open-loop controls forming the boundary of this set. In Section 4, we prove the properties of open-loop controls leading to the boundary of the two-dimensional set $\mathscr{G}(t_f,\mu)$. Section 5 presents relations that allow us to numerically construct the boundary of the reachable set $\mathscr{G}(t_f,\mu)$ under the integral constraint. Examples of constructing the reachable set $\mathscr{G}(t_f,\mu)$ are given in Section 6. There we also consider a comparison with the two-dimensional reachable sets under the geometric constraint.

2. Statement of the Problem

Let the motion of a controlled object on a plane be described by a system of differential equations

$$\dot{x}=\cos\varphi,\quad \dot{y}=\sin\varphi,\quad \dot{\varphi}=u. \tag{2.1}$$

Here x,y are the coordinates of the geometric position, φ is the inclination angle of the velocity vector counted counterclockwise from the positive direction of the axis x. The speed value is equal to unity. We assume the initial time t_0 to be equal to zero. The initial values $x(t_0),y(t_0),\varphi(t_0)$ are also considered to be zero. Admissible open-loop controls are measurable square-integrable functions $u(\cdot)$ that satisfy the constraint (1.1).

The reachable set $\mathscr{G}(t_f,\mu)$, where $t_f>t_0$, is the set of all points $(x,y)^{\mathsf{T}}$, to each of which system (2.1) can be transferred at the instant t_f from the initial phase state $(x(t_0),y(t_0),\varphi(t_0))^{\mathsf{T}}=(0,0,0)^{\mathsf{T}}$ using some admissible control $u(\cdot)$.

The purpose of the paper is to study the set $\mathscr{G}(t_f,\mu)$.

Let ∂ be a set boundary symbol. For the sake of brevity, we will use $z=(x,y,\varphi)^{\mathsf{T}}$. By the symbol $z^0(t_f)$, we denote the point on $\partial G(t_f,\mu)$ generated by the control $u(t)\equiv 0$.

3. Some Information about the Three-dimensional Reachable Set

When constructing the two-dimensional reachable set $\mathscr{G}(t_f,\mu)$ on the plane of the geometric coordinates x,y, we will rely on some facts known [13] for the three-dimensional reachable set $G(t_f,\mu)$ in the space of the coordinates x,y,φ. The definition of the set $G(t_f,\mu)$ is similar to the definition given for the set $\mathscr{G}(t_f,\mu)$ with the difference that at the instant t_f we take into account not only the coordinates $x(t_f),y(t_f)$ but also the coordinate $\varphi(t_f)$. It is convenient to assume that $\varphi\in(-\infty,\infty)$. The set $\mathscr{G}(t_f,\mu)$ is the projection of the set $G(t_f,\mu)$ onto the coordinate plane x,y.

By the symbol $G_\varphi(t_f,\mu)$, we will denote the two-dimensional section of the set $G(t_f,\mu)$ at fixed φ. The extreme values φ, for which $G_\varphi(t_f,\mu)\neq\varnothing$, are determined by the quantities $\varphi=\pm\varphi_{\max}$, where $\varphi_{\max}=\sqrt{t_f\mu}$. For such values φ, the set $G_\varphi(t_f,\mu)$ is single-pointed and is generated, accordingly, by the constant controls $u(t)\equiv\sqrt{\mu/t_f}$ and $u(t)\equiv-\sqrt{\mu/t_f}$.

3.1. **Properties of symmetry.** Let us list the following easily provable properties of symmetry for three-dimensional and two-dimensional reachable sets. Properties 1 – 3 refer to three-dimensional sets $G(t_f,\mu)$. They are presented in work [13]. Properties 4 and 5 are related to two-dimensional sets $\mathscr{G}(t_f,\mu)$. They follow from the properties 1 and 3 using the fact that any two-dimensional set $\mathscr{G}(t_f,\mu)$ can be represented as the union by φ of all φ-sections $G_\varphi(t_f,\mu)$ of the three-dimensional set $G(t_f,\mu)$.

1) Let the values $t_f^{(1)}$, $\mu^{(1)}$ and $t_f^{(2)}$, $\mu^{(2)}$ be such that $t_f^{(1)}\mu^{(1)} = t_f^{(2)}\mu^{(2)}$. Then the domains by φ of the sets $G(t_f^{(1)},\mu^{(1)})$ and $G(t_f^{(2)},\mu^{(2)})$ coincide, and for any φ the following relation holds:

$$G_\varphi(t_f^{(2)},\mu^{(2)}) = \alpha\, G_\varphi(t_f^{(1)},\mu^{(1)}), \quad \alpha = t_f^{(2)}/t_f^{(1)} = \mu^{(1)}/\mu^{(2)}.$$

2) Any φ-section $G_\varphi(t_f,\mu)$ is mirror symmetric about the auxiliary axis X. The axis X is drawn through the origin of coordinates x,y at an angle $\varphi(t_f)/2$ to the direction of the axis x. The angle is counted counterclockwise.

This symmetry property is proven by considering a "reverse" control: if some control $u(\cdot)$ at time t_f leads to the phase state $(x,y,\varphi)^\mathsf{T}$, then the control $u^\#(t) = u(t_f - t)$ (called reverse) leads to such phase state $(x^\#,y^\#,\varphi)^\mathsf{T}$, for which the points $(x,y)^\mathsf{T}$, $(x^\#,y^\#)^\mathsf{T}$ are mirror symmetric to each other about the axis X.

3) There is a symmetry of φ-sections for positive and negative values φ. Namely, the φ-section $G_{\overline{\varphi}}(t_f,\mu)$ at $\overline{\varphi} < 0$ is related to the φ-section $G_{\widehat{\varphi}}(t_f,\mu)$, where $\widehat{\varphi} = -\overline{\varphi}$, by the mirror reflection with respect to the axis x.

4) From the property 1, it follows that if $t_f^{(1)}$, $\mu^{(1)}$ and $t_f^{(2)}$, $\mu^{(2)}$ are such that $t_f^{(1)}\mu^{(1)} = t_f^{(2)}\mu^{(2)}$, then

$$\mathscr{G}(t_f^{(2)},\mu^{(2)}) = \alpha\mathscr{G}(t_f^{(1)},\mu^{(1)}), \quad \alpha = t_f^{(2)}/t_f^{(1)} = \mu^{(1)}/\mu^{(2)}.$$

5) Property 3 leads to the mirror symmetry of the set $\mathscr{G}(t_f,\mu)$ relative to the axis x.

3.2. **Pontryagin maximum principle.** Let us write down the Pontryagin maximum principle (PMP) used to analyze φ-sections of the three-dimensional reachable set $G(t_f,\mu)$. Here we repeat the main computations from work [13].

1) In work [11], it is established that any open-loop control leading system (2.1) to the boundary of the set $G(t_f,\mu)$ and different from identically equal to zero satisfies the PMP for problems of minimizing functional (1.2). With that, the minimum value of the functional on the motions of system (2.1) is equal to μ.

Let $u(\cdot)$ be an open-loop control not identically zero and $(x(\cdot),y(\cdot),\varphi(\cdot))^\mathsf{T}$ be the corresponding motion of system (2.1) on the interval $[t_0,t_f]$. The differential equations of the adjoint system have the form

$$\dot\psi_1 = 0, \quad \dot\psi_2 = 0, \quad \dot\psi_3 = \psi_1\sin\varphi(t) - \psi_2\cos\varphi(t). \tag{3.1}$$

The PMP means that if $u(\cdot)$ is a minimizing control, then there is a non-zero solution of system (3.1), $(\psi_1(\cdot),\psi_2(\cdot),\psi_3(\cdot))^\mathsf{T}$, for which the equality

$$u(t) = \psi_3(t)/2 \tag{3.2}$$

holds almost everywhere on $[t_0,t_f]$. In what follows, we assume that the control satisfying the PMP is continuous.

The functions $\psi_1(\cdot)$ and $\psi_2(\cdot)$ are constants. Let us denote them as ψ_1 and ψ_2. If $\psi_1 = 0$ and $\psi_2 = 0$, then $\psi_3(t) \equiv \text{const} \neq 0$. Therefore, in this case $u(t) \equiv \text{const} = \pm\sqrt{\mu/t_f}$. Such constant controls determine the extreme one-point φ-sections of the set $G_\varphi(t_f,\mu)$.

Now let at least one of the numbers ψ_1, ψ_2 be not equal to zero. Then, due to (2.1) and (3.1), we have

$$\psi_3(t) = \psi_1 y(t) - \psi_2 x(t) + C. \tag{3.3}$$

Hence, $\psi_3(t) = 0$ if and only if the point $(x(t), y(t))^\mathsf{T}$ of the geometric position of system (2.1) at time t under chosen $u(\cdot)$ satisfies the equation

$$\psi_1 y - \psi_2 x + C = 0 \tag{3.4}$$

of the straight switching line (SSL).

Let us denote $\chi = (-\psi_2, \psi_1)^\mathsf{T}$. We will call positive one of the two open half-planes defined by the SSL, where the vector χ is directed. In it, due to (3.2) and (3.4), we obtain $u(t) > 0$. We consider the opposite half-plane to be negative. In it, we have $u(t) < 0$. For points $(x(t), y(t))^\mathsf{T}$ on the SSL, the control $u(t)$ is zero. We choose the direction on the SSL so that it coincides with the direction of the vector $(\psi_1, \psi_2)^\mathsf{T}$, i.e., with the direction of the vector χ rotated by the angle $\pi/2$ clockwise (Fig. 1).

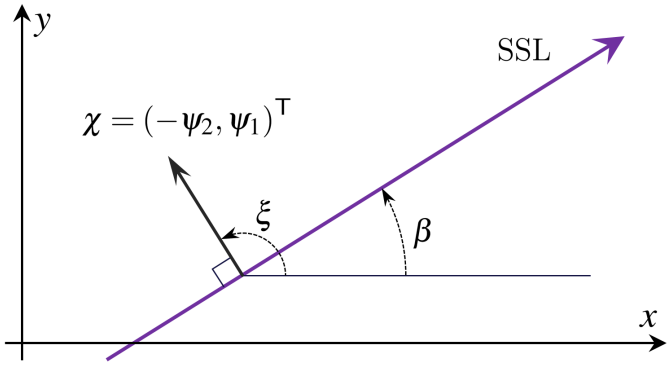

FIGURE 1. Explanation of notations χ, ξ, β

Supplementing systems (2.1) and (3.1) with relation (3.2), we arrive to a closed system of differential equations, for which the standard conditions of the existence and uniqueness theorems are satisfied. Therefore, in particular, there cannot be motions on the plane x, y that would approach the SSL tangentially in a finite time. Similarly, there cannot be motions that leave the SSL after some motion along it. It is only possible to cross the SSL under a non-zero angle or to exit from it at the initial instant (accordingly, to enter at the last instant) at a non-zero angle. Taking, in addition to the fixed initial condition $z(t_0) = 0$, the values ψ_1, ψ_2, $\psi_3(t_0)$, we obtain a set of motions $t \to z(t)$ necessarily containing all the motions leading to $\partial G(t_f, \mu)$.

2) Taking into account (3.2), we have

$$\ddot{\varphi}(t) = \frac{\dot{\psi}_3(t)}{2} = \frac{\psi_1}{2}\sin\varphi(t) - \frac{\psi_2}{2}\cos\varphi(t) = \rho\left(\frac{\psi_1}{2\rho}\sin\varphi(t) - \frac{\psi_2}{2\rho}\cos\varphi(t)\right).$$

Here $\rho = \sqrt{\left(-\frac{\psi_2}{2}\right)^2 + \left(\frac{\psi_1}{2}\right)^2}$. Let us define the angle ξ: $\cos\xi = -\frac{\psi_2}{2\rho}$, $\sin\xi = \frac{\psi_1}{2\rho}$. By agreement, we count angles from the direction of the axis x counterclockwise. We obtain that ξ is the angle of inclination of the vector χ with respect to the axis x.

Continuing the relation for $\ddot{\varphi}$, we have

$$\ddot{\varphi}(t) = \rho\left(\sin\xi\sin\varphi(t) + \cos\xi\cos\varphi(t)\right) = \rho\cos\left(\varphi(t) - \xi\right).$$

Let us put $\beta = \xi - \pi/2$. The angle β is considered between the direction of the axis x and the direction of the SSL (Fig. 1). Since $\varphi(t_0) = 0$, we can say that β is the angle between the direction of the velocity vector at the initial instant and the direction of the SSL. We have

$$\cos(\varphi(t) - \xi) = \cos\left(\varphi(t) - \beta - \frac{\pi}{2}\right) = \sin(\varphi(t) - \beta).$$

Therefore,

$$\ddot{\varphi}(t) = \rho \sin(\varphi(t) - \beta). \tag{3.5}$$

Thus, when we analyze extremal motions with the help of the PMP, then a consideration of the constants ψ_1, ψ_2, $\psi_3(0)$ can be replaced by a consideration of the values ρ, β and $\dot{\varphi}(0) = \psi_3(0)/2$.

3) Multiplying relation (3.5) by $2\dot{\varphi}(t)$ (by analogy with [15, p. 282]), we have

$$\frac{d(\dot{\varphi}(t))^2}{dt} = 2\dot{\varphi}(t)\ddot{\varphi}(t) = 2\dot{\varphi}(t)\rho \sin(\varphi(t) - \beta).$$

From here,

$$(\dot{\varphi}(t))^2 = c_* - 2\rho \cos(\varphi(t) - \beta). \tag{3.6}$$

For $\dot{\varphi}(t) \neq 0$, we obtain

$$\dot{\varphi}(t) = \pm\sqrt{c_* - 2\rho \cos(\varphi(t) - \beta)}. \tag{3.7}$$

We use this formula on intervals of motion where $\dot{\varphi}(t) \neq 0$. The sign "+" corresponds to control $u(t) > 0$, the sign "−" means that $u(t) < 0$. The constants C in (3.4) and c_* in (3.6) are related by the relation

$$c_* = 2\rho \cos\beta + C^2/4. \tag{3.8}$$

Indeed, given (3.2) and (3.3), we write

$$\dot{\varphi}(t) = \frac{\psi_3(t)}{2} = \frac{\psi_1 y(t) - \psi_2 x(t) + C}{2}.$$

By virtue of (3.7), we obtain

$$c_* - 2\rho \cos(\varphi(t) - \beta) = \frac{(\psi_1 y(t) - \psi_2 x(t) + C)^2}{4}.$$

At the initial instant t_0, we have $x(t_0) = y(t_0) = \varphi(t_0) = 0$. It gives (3.8). If at some instant t the point $(x(t), y(t))^{\mathsf{T}}$ lies on the SSL, then

$$c_* = 2\rho \cos\beta'. \tag{3.9}$$

Here $\beta' = \beta - \varphi(t)$ is the inclination angle of the velocity vector of system (2.1) at the instant t with respect to the direction of the SSL counted counterclockwise from the direction of the velocity vector. From (3.7), we have

$$dt = \frac{d\varphi}{\pm\sqrt{c_* - 2\rho \cos(\varphi - \beta)}}. \tag{3.10}$$

Formula (3.10) allows us to replace the integration over t by the integration over φ in half-planes with constant sign of the control.

4) When constructing motions that satisfy the PMP, we use the straight switching line. If a motion crosses the SSL at some point, then after this point it follows a trajectory that is centrally symmetric (relative to the point of intersection) to the trajectory part before the intersection instant. The following statement indicates some additional (directly following from the PMP)

properties of motions passing through the SSL. This statement was given in a more general formulation in [13, Proposition 5.1].

Proposition 3.1. *Let the motion $z(\cdot)$ of system (2.1) on the interval $[t_0,t_f]$ be generated by a continuous control $u(\cdot)$ (not identically zero) and the PMP be fulfilled. Then the control $u(\cdot)$ changes sign no more than a finite number of times. Moreover:*

a) points of the geometric position of system (2.1) on the plane x,y at the instants of sign change of the control $u(\cdot)$ lie on the SSL;

b) if $z(\cdot)$ is such that the motion $(x(\cdot),y(\cdot))^{\mathsf{T}}$ hits the SSL at least three times, then the time between any adjacent instants of being on the SSL is the same; the corresponding increment of the angle in absolute value is also the same;

c) if $z(\cdot)$ is such that the motion $(x(\cdot),y(\cdot))^{\mathsf{T}}$ hits the SSL at least once, then the accumulated angle on each interval of constancy of the control sign is less than 2π in absolute value.

3.3. **Types of controls leading to the boundary of the three-dimensional reachable set.** The work [13] shows that to construct the boundary of the three-dimensional reachable set $G(t_f,\mu)$, it is sufficient to use six types U_1-U_6 of continuous open-loop controls $u(\cdot)$ with no more than two instants of control sign change. The equality $u(t)=0$ means that the point on the extremal motion under consideration is on the SSL at the instant t.

Let us list the types of open-loop controls. The type U_1 is characterized by the fact that $u(t)>0$ on the entire interval $[t_0,t_f]$. Similarly, the type U_4 is determined with positive control replaced by negative control. The type U_3 has one instant of changing the control sign on (t_0,t_f) with the sign "+" first, then "−". Controls for which $u(t)>0$, $t\in(t_0,t_f)$, but $u(t_0)=0$ or $u(t_f)=0$ are also assumed to be included in U_3. Similarly for U_2: one instant of change of sign from "−" to "+". The type U_6 is specified by two instants of sign change on (t_0,t_f) and the sequence $-$, $+$, $-$. The type U_5 also has two instants of control sign change on (t_0,t_f), but the sequence $+$, $-$, $+$ is used.

For controls belonging to the types U_6 and U_5, the following statement is true [13] related to the duration of the middle interval of control.

Lemma 3.2. *Let the motion $z(\cdot)$ of system (2.1) on the interval $[t_0,t_f]$ be generated by a continuous control $u(\cdot)$ satisfying the PMP with two instants t_1, t_2 of changes of the control sign, and $t_0<t_1<t_2<t_f$. Suppose that*

$$(t_1-t_0)+(t_f-t_2)>(t_2-t_1). \tag{3.11}$$

Then $z(t_f)\in\operatorname{int}G(t_f)$.

Using this statement, the following theorem is proved in [13].

Theorem 3.3. *For any point $z(t_f)\neq z^0(t_f)$ on $\partial G(t_f,\mu)$, there is a continuous control going to this point, satisfying the PMP and belonging to one of the types U_1-U_6. There are no other variants of control leading to the boundary. If $\varphi(t_f)>0$, then in the list of six types we leave only four: U_1, U_2, U_3, U_6. In the case $\varphi(t_f)<0$, we restrict ourselves by the four types U_2, U_3, U_4, U_5. If $\varphi(t_f)=0$, we leave the types U_2, U_3, U_5, U_6; with that, controls of the types U_5 and U_6 generate the same set of points.*

Figure 2 shows an example of the three-dimensional reachable set for $t_f=(1.5\pi)^2$, $\mu=1$. The three-dimensional set is shown from two points of view. The parts of the boundary corresponding to different types of control are marked in color.

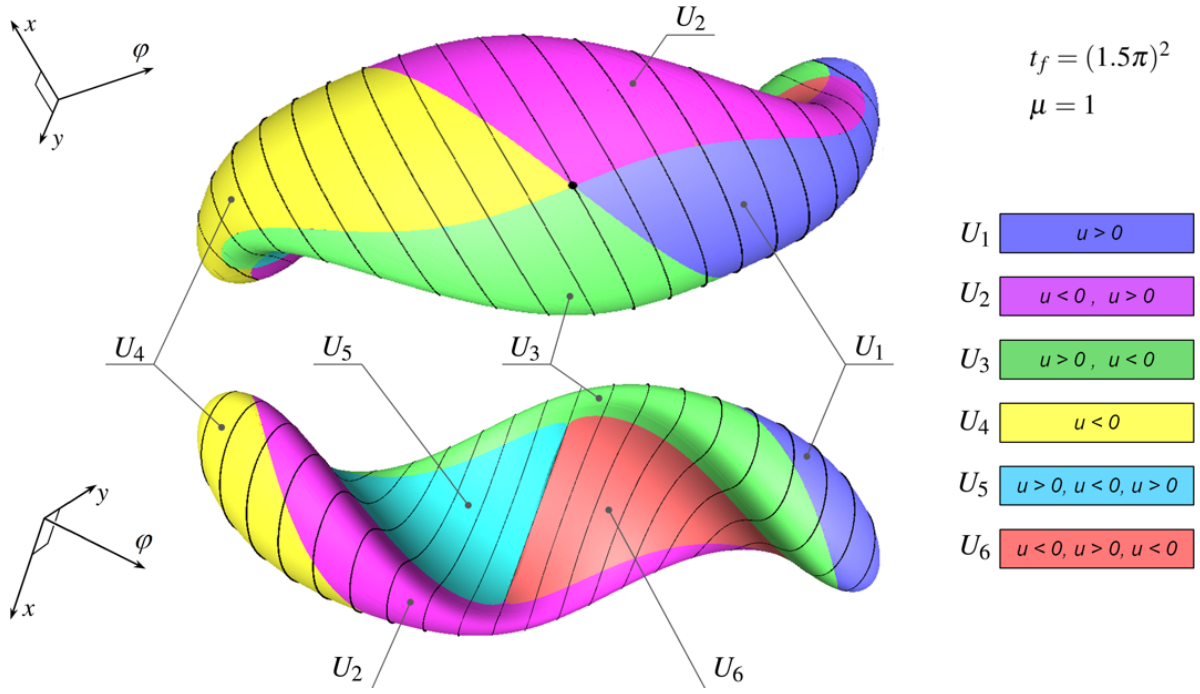

FIGURE 2. Three-dimensional reachable set for $t_f = (1.5\pi)^2$, $\mu = 1$ from two points of view

We will use the results of this section to analyze controls leading to the boundary of the two-dimensional set $\mathscr{G}(t_f, \mu)$.

4. Structure of Controls Leading to the Boundary of the Set $\mathscr{G}(t_f, \mu)$

Since the two-dimensional set $\mathscr{G}(t_f, \mu)$ is the projection of the three-dimensional set $G(t_f, \mu)$ onto the plane x, y, then any motion of system (2.1) going to the boundary of the set $\mathscr{G}(t_f, \mu)$ leads to the boundary of the set $G(t_f, \mu)$, i.e., satisfies Theorem 3.3. When considering the boundary of the set $\mathscr{G}(t_f, \mu)$, we will use the edge condition $\psi_3(t_f) = 0$ established in paper [14]. The condition $\psi_3(t_f) = 0$ means that $u(t_f) = 0$. Thus, the motion arrives at the instant t_f on the switching line.

4.1. **Number of instants of control sign change.** The presence of the edge condition $u(t_f) = 0$ excludes, when constructing the boundary of the set $\mathscr{G}(t_f, \mu)$, open-loop controls related to the types U_1 and U_4. Consider an open-loop control $u(\cdot)$ of the type U_6 or U_5. By definition, the corresponding motion crosses the SSL at two instants t_1 and t_2, where $t_0 < t_1 < t_2 < t_f$. With that, by Lemma 3.2, the inequality $(t_2 - t_1) \geq (t_1 - t_0) + (t_f - t_2)$ holds. If we assume that $u(t_f) = 0$, then taking into account Proposition 3.1b, we have $(t_f - t_2) = (t_2 - t_1)$. Since $(t_1 - t_0) > 0$, we obtain the contradiction. Thus, open-loop controls of the types U_6 and U_5 do not lead to the boundary of the set $\mathscr{G}(t_f, \mu)$.

As a result, when studying the boundary of the set $\mathscr{G}(t_f, \mu)$ (except for the point corresponding to the special control $u(t) \equiv 0$), one must use only controls of the types U_3 and U_2 satisfying the edge condition $u(t_f) = 0$.

The following statement is true.

Theorem 4.1. *The special control $u(t)\equiv 0$ leads to the boundary of the set $\mathscr{G}(t_f,\mu)$. All other points of the boundary of the reachable set $\mathscr{G}(t_f,\mu)$ are formed using continuous controls, which satisfy the PMP, the condition $u(t_f)=0$ and have no more than one instant of sign change on (t_0,t_f). There are no other open-loop control variants leading to the boundary.*

Note that for the Dubins car with the geometric constraint $|u(t)|\le\mu$ on control, a similar statement is valid (see [4, p. 211, Theorem 3]). Namely, any extremal control leading to the boundary of the two-dimensional reachable set on the plane x,y is a piecewise-constant with at most one switching instant.

4.2. **Eliminating useless extremal motions.** Below we formulate and prove three clarifying lemmas. They provide simple criteria for rejecting motions that satisfy the conditions of Theorem 4.1 but lead into the interior of the set $\mathscr{G}(t_f,\mu)$.

Lemma 4.2 says that trajectories going to $\partial\mathscr{G}(t_f,\mu)$ have no self-intersections. By virtue of Lemma 4.4, for the motions leading to $\partial\mathscr{G}(t_f,\mu)$ with $\varphi(t_f)\neq 0$, the inequality $y(t_f)\cdot\varphi(t_f)\ge 0$ holds. For the case of the geometric control constraint, a similar property was also hold true (see [4, pp. 211–212]). Lemma 4.7 allows, under the conditions of Theorem 4.1, to restrict ourselves to the values $\varphi(t_f)\in(-2\pi,2\pi)$.

The proofs of the lemmas are very simple but are based on consideration of the geometry for various variants of extremal motions. Therefore, the proofs are accompanied by a large number of figures.

Under proving Lemmas 4.2 and 4.4, we use the standard method of constructing the auxiliary motion of system (2.1), which comes out from the same initial phase point $(x(t_0),y(t_0),\varphi(t_0))^{\mathsf{T}}$, as the original motion, and arrives at the instant t_f to the same final geometric point $\big(x(t_f),y(t_f)\big)^{\mathsf{T}}$ (but not necessarily with the same value of $\varphi(t_f)$ of the angular variable). Therewith, the auxiliary control is constructed in such a way that, unlike the original control, it does not satisfy the PMP. So, the final geometric point $\big(x(t_f),y(t_f)\big)^{\mathsf{T}}$ does not lie on $\partial\mathscr{G}(t_f,\mu)$.

When considering Lemmas 4.2 and 4.7, we use the term "Euler lemniscate". This is a closed curve (bow, infinity sign), which is a special case of the Euler elastica and is described in his book [5, pp. 262 – 263]. The Euler lemniscate has an angle at the nodal point of approximately 81°. Thus, the Euler lemniscate differs from the well-known Bernoulli lemniscate, for which such an angle is equal to 90°. It is the Euler lemniscate that is used to analyze the reachable set for the Dubins car.

Lemma 4.2. *Let a control $u(\cdot)$ satisfy the conditions of Theorem 4.1, but the corresponding trajectory $(x(\cdot),y(\cdot))^{\mathsf{T}}$ have self-intersection, i.e., there exist instants $t_*<t^*$ in (t_0,t_f) such that $(x(t_*),y(t_*))^{\mathsf{T}}=(x(t^*),y(t^*))^{\mathsf{T}}$. Then $\big(x(t_f),y(t_f)\big)^{\mathsf{T}}\in\operatorname{int}\mathscr{G}(t_f,\mu)$.*

Proof. 1) Suppose that the control $u(\cdot)$ does not change sign on the interval (t_0,t_f). Due to self-intersection, there is a loop on the generated trajectory (Fig. 3). We draw a tangent to this loop through the point $\big(x(t_f),y(t_f)\big)^{\mathsf{T}}$. Then we mirror the arc of the original trajectory between the tangent point $\widehat{S}=\big(x(\widehat{t}),y(\widehat{t})\big)^{\mathsf{T}}$ and the end point $S_2=\big(x(t_f),y(t_f)\big)^{\mathsf{T}}$ relative to the constructed tangent. Let us define an auxiliary control $\widetilde{u}(\cdot)$ so that it would be coincided with the original one up to the instant $\widehat{t}$ and would be generate a mirror-image trajectory on $[\widehat{t},t_f]$. The latter means that $\widetilde{u}(t)=-u(t)$ for $t\in[\widehat{t},t_f]$. The auxiliary control $\widetilde{u}(\cdot)$ does not satisfy the PMP because

at the instant $\widehat{t}$ it is discontinuous: the control $\widetilde{u}(\cdot)$ jumps from $\widetilde{u}(\widehat{t}-0)=u(\widehat{t}-0)=u(\widehat{t})$ to $\widetilde{u}(\widehat{t}+0)=-u(\widehat{t}+0)=-u(\widehat{t})$.

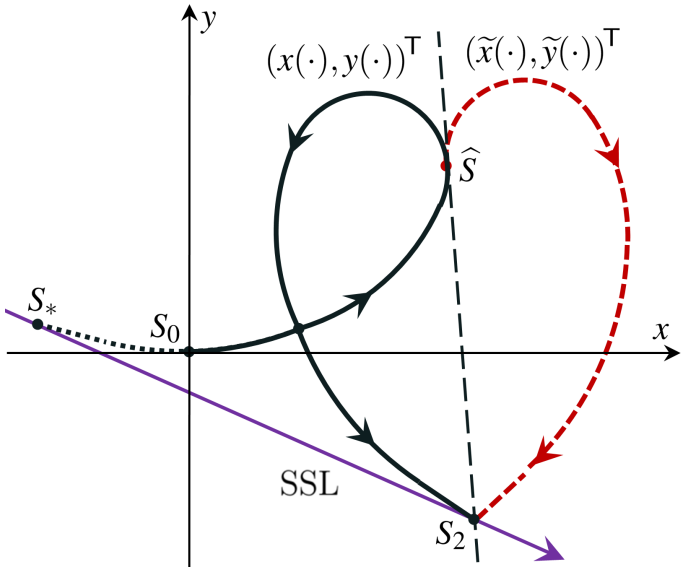

FIGURE 3. Explanation to the item 1) of Lemma 4.2 proof.
Control $u(\cdot)$ does not change sign on the interval (t_0,t_f)

2) Let the control $u(\cdot)$ change sign at some instant $t_1\in(t_0,t_f)$. If there is a self-intersection, then there are one or two self-intersection points. In the both cases, there is a self-intersection point for which the instants t_*,t^* are located on the interval (t_1,t_f) (Fig. 4). We draw the tangent to such a loop through the point $S_2=\big(x(t_f),y(t_f)\big)^{\mathsf{T}}$. Then we construct an auxiliary motion. Its mirrored part is shown in Fig. 4 by red dashed line. The control implementing the auxiliary motion is discontinuous at the instant of passing the point $\widehat{S}$. Therefore, it does not satisfy the PMP. □

Remark 4.3. The trajectories shown in Figs. 5 and 6 do not formally satisfy the conditions of Lemma 4.2. Namely, the definition of self-intersection is not satisfied here. But the proof made in Lemma 4.2 actually covers these cases as well.

Lemma 4.4. *Let $u(\cdot)$ be an open-loop control that satisfies the conditions of Theorem 4.1. Let us assume that the inequalities $\varphi(t_f)>0$, $y(t_f)<0$ or $\varphi(t_f)<0$, $y(t_f)>0$ are realized for the corresponding motion. Then $\big(x(t_f),y(t_f)\big)^{\mathsf{T}}\in\operatorname{int}\mathscr{G}(t_f,\mu)$.*

Proof. For definiteness, we consider the variant $\varphi(t_f)>0$, $y(t_f)<0$.

1) Let the control $u(\cdot)$ be such that the emerging trajectory has self-intersection. Then, by Lemma 4.2, we get $\big(x(t_f),y(t_f)\big)^{\mathsf{T}}\in\operatorname{int}\mathscr{G}(t_f,\mu)$.

2) Let us now assume that there are no self-intersections.

2a) Consider the case when the control $u(\cdot)$ on the interval (t_0,t_f) does not change sign, i.e., $u(t)>0$, $t\in(t_0,t_f)$. With that $u(t_f)=0$, $y(t_f)<0$. Let us draw through the point $S_2=\big(x(t_f),y(t_f)\big)^{\mathsf{T}}$ the tangent to the initial part of the trajectory above the axis x. Such a tangent exists and is unique. Let us denote by the symbol $\widehat{S}$ the point of tangency and by the symbol $\widehat{t}$

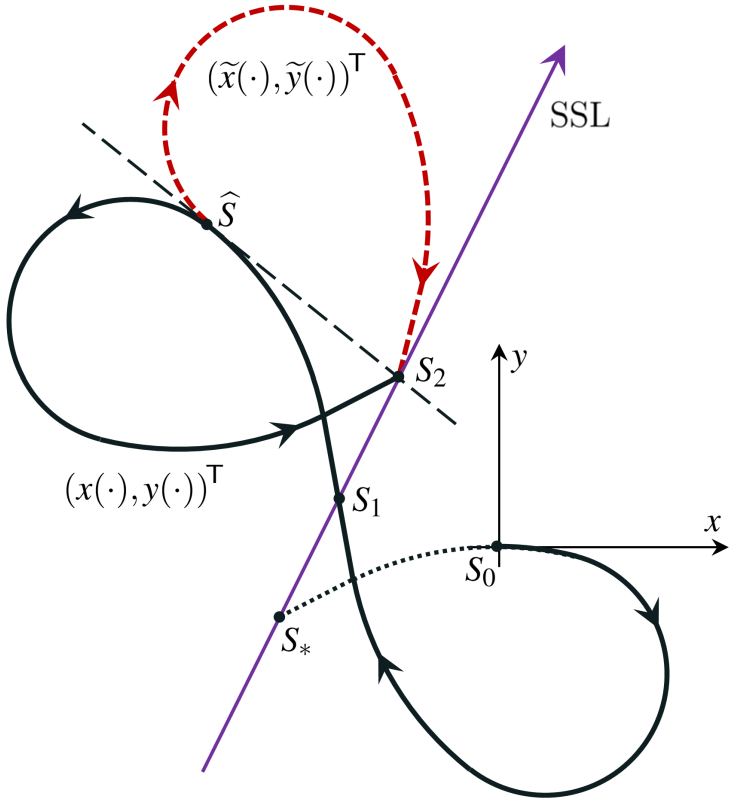

FIGURE 4. Explanation to the item 2) of the Lemma 4.2 proof. Control $u(\cdot)$ changes sign on the switching straight line

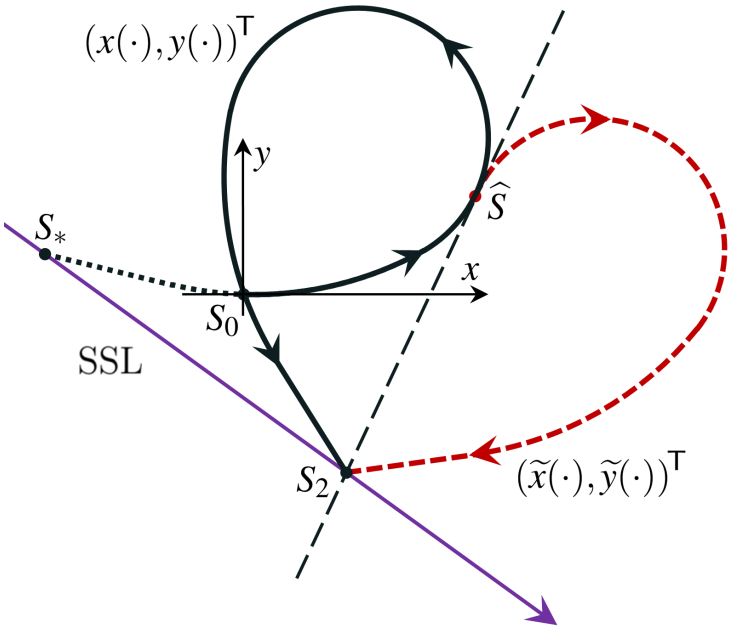

FIGURE 5. Explanation to Remark 4.3. The loop on the trajectory begins at the starting point S_0

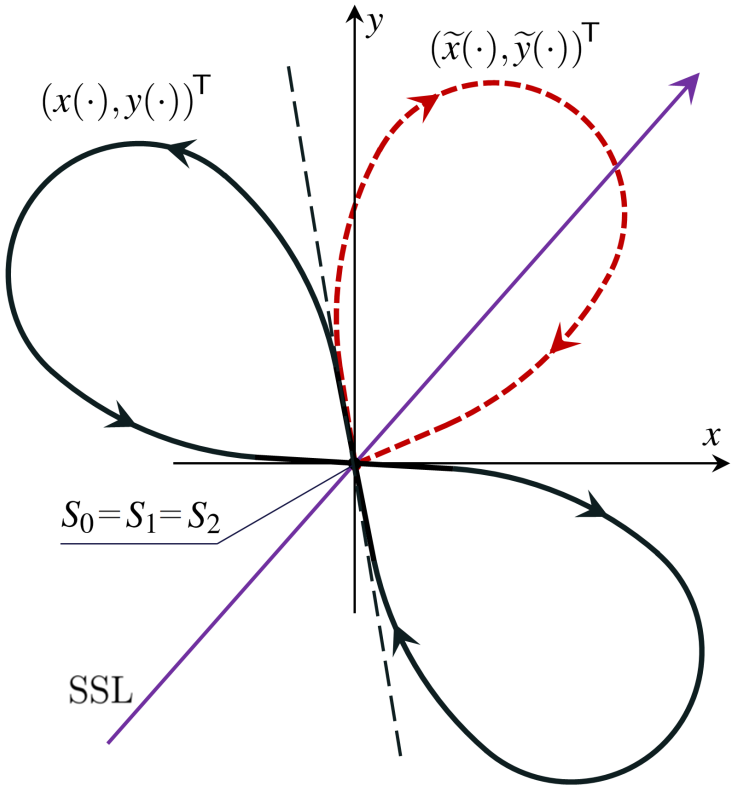

FIGURE 6. Explanation to Remark 4.3. The motion goes on the Euler lemniscate. Points S_0, S_1 and S_2 coincide

the instant of passing this point. We mirror the part of the original trajectory on $[\widehat{t},t_f]$ relative to the tangent (red dashed line in Fig. 7). Consider the auxiliary motion $(\widetilde{x}(\cdot),\widetilde{y}(\cdot),\widetilde{\varphi}(\cdot))^{\mathsf{T}}$, which coincides with the original one on $[0,\widehat{t}\,]$ and further goes on $(\widehat{t},t_f]$ in the x,y plane along the reflected trajectory (with a change in the control sign relative to the original one). By construction, the equality $(x(t_f),y(t_f))^{\mathsf{T}}=(\widetilde{x}(t_f),\widetilde{y}(t_f))^{\mathsf{T}}$ holds. Since at the point $\widehat{S}$ of tangency we have $u(\widehat{t}\,)>0$, then we obtain $\widetilde{u}(\widehat{t}+0)=-u(\widehat{t}\,)<0$ on the auxiliary motion. Therefore, the control at the instant $\widehat{t}$ is discontinuous for the auxiliary motion. So, it does not satisfy the PMP. Hence, $(x(t_f),y(t_f))^{\mathsf{T}}=(\widetilde{x}(t_f),\widetilde{y}(t_f))^{\mathsf{T}}\in\operatorname{int}\mathscr{G}(t_f,\mu)$.

2b) Suppose that the control $u(\cdot)$ changes sign at some instant $t_1\in(t_0,t_f)$. In addition, we assume $\varphi(t_f)>0$. Then $u(t)<0$ on $[t_0,t_1)$ and $u(t)>0$ on (t_1,t_f). Since there are no self-intersections, the point S_1 of crossing the SSL at the instant t_1 is located on the SSL (taking into account its direction) not farther from the point S_2 of hitting the SSL at the instant t_f (Figs. 8, 9, 10).

Let us consider two typical variants: $S_2\neq S_1$ and $S_2=S_1$. In each of them, the motion begins at the point S_0, hits the SSL at the time t_1 (the point S_1) and ends at the SSL at the time t_f (the point S_2). We extend the extremal trajectory of the first part in backward time from the point S_0 to hitting the SSL at the point S_* (marked by green dotted line). The curve from the point S_* to the point S_1 is centrally symmetric to the second part from S_1 to S_2 of the original curve. We investigate these two variants separately.

2b1) We consider that $S_2\neq S_1$ (Fig. 8). We draw a tangent from the point S_2 to the arc starting at the point S_* and ending at the point S_1. Let $\widehat{S}$ be the point of tangency.

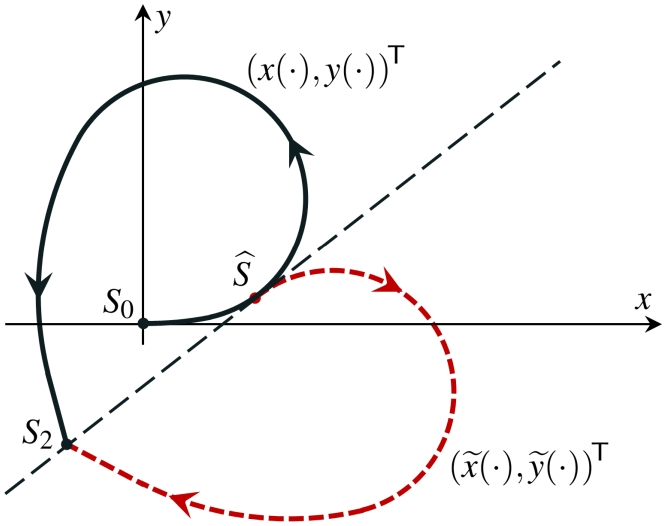

FIGURE 7. Explanation to the item 2a) of the Lemma 4.4 proof

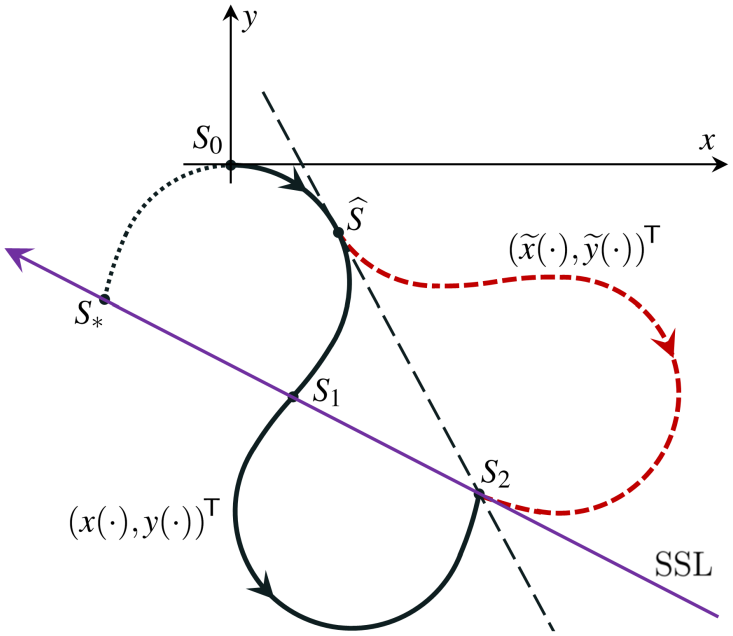

FIGURE 8. Explanation to the item 2b1) of the Lemma 4.4 proof. The starting point S_0 is on the arc $[S_*, \widehat{S})$

If the point S_0 lies on the arc $(S_*, \widehat{S})$, then, using the reflection relative to the tangent, we construct an auxiliary motion $(\widetilde{x}(\cdot),\widetilde{y}(\cdot))^{\mathsf{T}}$. It differs from the original one after the instant $\widehat{t}$ and arrives at the instant t_f at the same point S_2. The control for the auxiliary motion does not satisfy the PMP. Therefore, $S_2 = (x(t_f),y(t_f))^{\mathsf{T}} \in \operatorname{int}\mathscr{G}(t_f,\mu)$.

Now we suppose that $S_0 \in [\widehat{S},S_1)$ (Fig. 9). Consider the axis x drawn through the point S_0 tangent to the curve $[\widehat{S},S_1)$ in the direction of the motion. The point S_2 in this case lies either above the axis x (if $S_0 \in (\widehat{S},S_1)$) or on this axis (if $S_0 = \widehat{S}$). We come to the contradiction with the condition of the lemma.

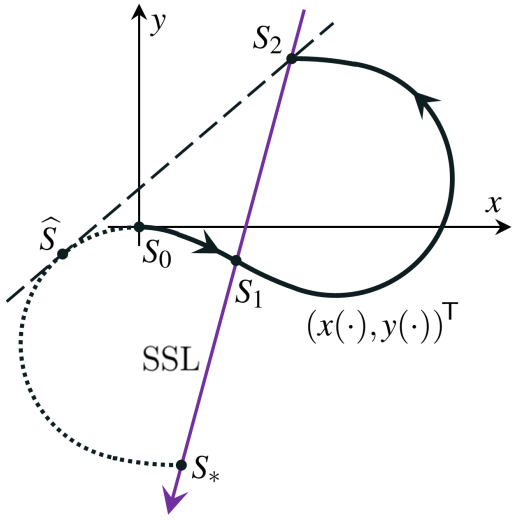

FIGURE 9. Explanation to the item 2b1) of the Lemma 4.4 proof. The starting point S_0 is on the arc $[\widehat{S}, S_1)$

2b2) Let us assume that $S_2 = S_1$ (Fig. 10). In this case, the motion goes along the Euler lemniscate $S_*S_1S_2$. Let us draw a tangent through the point S_1 to the trajectory in the direction of the motion at time t_1. We use this tangent to construct (by reflection) an auxiliary motion that coincides with the original one up to the instant t_1 and differs from it on the interval $(t_1, t_f]$. In Fig. 10, the trajectory of the auxiliary motion on the interval $(t_1, t_f]$ is shown by the red dashed line.

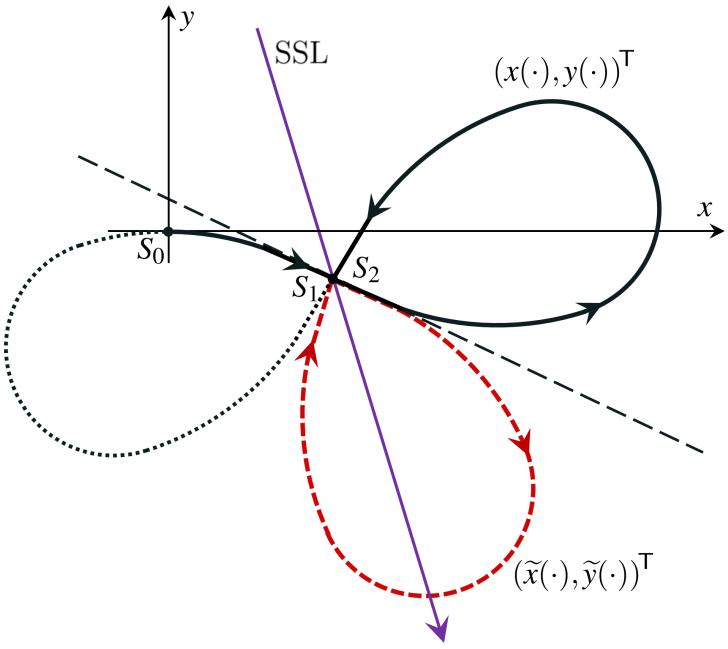

FIGURE 10. Explanation to the item 2b2) of the Lemma 4.4 proof. The points S_1 and S_2 coincide

The resulting auxiliary motion at the instant t_f arrives to the same point S_2 on the plane x, y as the original motion. But at the same time, the corresponding control $\widetilde{u}(\cdot)$ does not change sign

on the interval (t_0,t_f) although it becomes zero at the instant t_1. Therefore, it does not satisfy the PMP and, as a consequence, leads to $\mathrm{int}\mathscr{G}(t_f,\mu)$. □

The following facts additionally follow from the proof of Lemma 4.4.

Remark 4.5. The formulation of Lemma 4.4 does not take into account the case where $\varphi(t_f)=0$ and the motion under consideration is different from identically equal to zero. For such a case, only two symmetrical variants are possible. In the first of them, $u(t)>0$ on (t_0,t_1) and $u(t)<0$ on (t_1,t_f). In the second, conversely, $u(t)<0$ on (t_0,t_1) and $u(t)>0$ on (t_1,t_f). With that, the initial point S_0, the point S_1 of the control sign change and the end point S_2 of the trajectory are located on the SSL.

If $S_0\neq S_1$ (and, hence, $S_1\neq S_2$), then this case is analogous to the case 2b1) considered in Lemma 4.4 proof when $S_0\in(\widehat{S},S_1)$. Therefore, $S_2\in\mathrm{int}\mathscr{G}(t_f,\mu)$. In the case $S_0=S_1=S_2$, the trajectory is the Euler lemniscate. The reasoning in 2b2) can be essentially repeated here. It follows that the extremal motion in the form of the Euler lemniscate leads to $\mathrm{int}\mathscr{G}(t_f,\mu)$.

Thus, when $\varphi(t_f)=0$, only a special motion with control $u(t)\equiv 0$ gives a point on the boundary of the set $\mathscr{G}(t_f,\mu)$.

Remark 4.6. If on the motion leading to the boundary of the set $\mathscr{G}(t_f,\mu)$ there is an instant of sign change, then the initial part of such a motion before the change of sign cannot exceed the angle π. Indeed, otherwise, the initial point S_0 belongs to the arc $[S_*,\widehat{S}\,)$ and, as noted in the proof of Lemma 4.4, the last point S_2 lies in $\mathrm{int}\mathscr{G}(t_f,\mu)$.

Lemma 4.7. *If for some extremal motion* $(x(\cdot),y(\cdot),\varphi(\cdot))^{\mathsf{T}}$ *the inequality* $\big|\varphi(t_f)\big|\geq 2\pi$ *is satisfied, then* $\big(x(t_f),y(t_f)\big)^{\mathsf{T}}\in\mathrm{int}\mathscr{G}(t_f,\mu)$.

Proof. The maximal value $\varphi=\varphi_{\max}$, at which $G_\varphi(t_f,\mu)\neq\varnothing$, is defined by the formula $\varphi_{\max}=\sqrt{t_f\cdot\mu}$. We assume that $\varphi_{\max}\geq 2\pi$.

Consider the case $\varphi(t_f)\in[2\pi,\varphi_{\max}]$. Suppose from the contrary that some admissible control $u(\cdot)$ realizing $\varphi(t_f)$ leads to the boundary of the set $\mathscr{G}(t_f,\mu)$. Then $u(t_f)=0$, and by virtue of Proposition 3.1c, the accumulated angle on each interval of constancy of the control sign is less than 2π in absolute value. Therefore, the angle $\varphi(t_f)$, which is accumulated over the entire interval $[t_0,t_f]$, is also less than 2π in absolute value. We got the contradiction.

Due to the symmetry of the φ-sections $G_\varphi(t_f,\mu)$ for positive and negative values φ (property 3 in Section 3.1), the assertion being proved is also true for $\varphi(t_f)\leq -2\pi$. □

5. Analysis of Controls Leading to the Boundary of the Set $\mathscr{G}(t_f,\mu)$

Having fixed t_f and μ, we take the value $\varphi(t_f)\in[-\varphi_{\max},\varphi_{\max}]$ as a parameter when describing the boundary of the set $\mathscr{G}(t_f,\mu)$. We emphasize that the value $\varphi_{\max}$ depends on t_f and μ.

1) Consider the case $\varphi(t_f)\in[0,\varphi_{\max})$. By virtue of Theorem 4.1, the boundary of the set $\mathscr{G}(t_f,\mu)$ can be generated, in addition to the special control $u(t)\equiv 0$, by controls only of the types U_3 and U_2 with the edge condition $u(t_f)=0$.

We divide controls of the type U_3 into three cases:

— control $u(t)$ is positive on (t_0,t_f);

— control $u(t)$ changes sign from $+$ to $-$ once on (t_0,t_f) and $u(t_0)>0$;

— control $u(t)$ changes sign from $+$ to $-$ once on (t_0,t_f) and $u(t_0)=0$.

We denote the set of controls related to the first case by $U^{(+)}$. For the second case, we have $u(t_0)>0$ and $u(t_f)=0$. Therefore, relying on the symmetry of the trajectory relative to the intersection point with the SSL (Section 3.1), we obtain $\varphi(t_f)<0$. Since this contradicts the assumption $\varphi(t_f)\in[0,\varphi_{\max})$, the second case is impossible. In the third case, we have $\varphi(t_f)=0$ by virtue of Proposition 3.1b. Based on Remark 4.5, we establish that such a control does not lead to the boundary of the reachable set $\mathscr{G}(t_f,\mu)$. Therefore, we also reject the third case.

For controls of the type U_2, we distinguish three similar cases:

— control $u(t)$ is negative on (t_0,t_f);

— control $u(t)$ changes sign from $-$ to $+$ once on (t_0,t_f) and $u(t_0)<0$;

— control $u(t)$ changes sign from $-$ to $+$ once on (t_0,t_f) and $u(t_0)=0$.

The first case is not suitable due to the fact that $\varphi(t_f)\geq 0$. We denote the set of controls related to the second case by $U^{(-,+)}$. We reject the third case (just like for controls of the type U_3).

Thus, in what follows, we will consider only the controls $U^{(+)}$ (belonging to the type U_3) and $U^{(-,+)}$ (of the type U_2). Only these controls can lead to the boundary of the set $\mathscr{G}(t_f,\mu)$ for $\varphi(t_f)\geq 0$.

2) When constructing the motions due to the $U^{(+)}$ controls, we will use relations (7.6), (7.7) from the paper [13], which were obtained for the type U_3 controls. In these relations, taking into account the edge condition $u(t_f)=0$ for controls $U^{(+)}$, we should put $\varphi_3=0$. Then in each formula there remains one integral:

$$t_f=\frac{1}{\sqrt{2\rho}}\int_0^{\varphi(t_f)}\frac{d\varphi}{\sqrt{\cos\beta'-\cos(\varphi+\beta')}}, \tag{5.1}$$

$$\mu=\sqrt{2\rho}\int_0^{\varphi(t_f)}\sqrt{\cos\beta'-\cos(\varphi+\beta')}\,d\varphi. \tag{5.2}$$

Here β' is the angle counted counterclockwise from the direction of the velocity vector of system (2.1) at the instant t_f to the direction of the SSL. The quantity ρ is a constant used in relation (3.5).

2a) We explain formula (5.1). Formula (5.2) is explained in a similar way.

Let us consider the motion due to the positive control $u(\cdot)$ on $[t_0,t_f)$. It finishes at the instant t_f on the SSL. The angle accumulated on $[t_0,t_f]$ is equal to $\varphi(t_f)$. Based on (3.10) and using the sign "+" in front of the root, we get

$$t_f=\int_0^{\varphi(t_f)}\frac{d\varphi}{\sqrt{c_*-2\rho\cos(\varphi-\beta)}}.$$

When calculating the integral, we make the substitution $\varphi'=\varphi(t_f)-\varphi$. Then $d\varphi'=-d\varphi$. The value $\varphi=0$ corresponds to $\varphi'=\varphi(t_f)$, and $\varphi=\varphi(t_f)$ is replaced by $\varphi'=0$. Introducing the notation $\beta'=\beta-\varphi(t_f)$, we obtain

$$t_f=\int_{\varphi(t_f)}^0\frac{-d\varphi'}{\sqrt{c_*-2\rho\cos(-\varphi'-\beta')}}=\int_0^{\varphi(t_f)}\frac{d\varphi'}{\sqrt{c_*-2\rho\cos(\varphi'+\beta')}}.$$

The value c_* is calculated using formula (3.9), i.e., $c_*=2\rho\cos\beta'$. Thus, the resulting integral has the form (5.1). In this case, the meaning of the angle β' is exactly what is indicated in the description of formula (5.1). The symbol φ', like φ in (5.1), denotes the variable of integration.

2b) By analogy with [13], writing the product $t_f \cdot \mu$, we eliminate ρ and obtain the relation

$$t_f \cdot \mu = \int_0^{\varphi(t_f)} \frac{d\varphi}{\sqrt{\cos\beta' - \cos(\varphi+\beta')}} \cdot \int_0^{\varphi(t_f)} \sqrt{\cos\beta' - \cos(\varphi+\beta')}\, d\varphi, \qquad (5.3)$$

connecting the parameters $\varphi(t_f)$ and β'. When investigating such an equation numerically for a fixed $\varphi(t_f)$ in the interval from 0 to some $\varphi^{(1)}(t_f)$, we obtain a unique solution (the value of β' depending on $\varphi(t_f)$). For $\varphi(t_f)$ in the range from $\varphi^{(1)}(t_f)$ to some $\varphi^{(2)}(t_f)$, we have two solutions (two values β' depending on $\varphi(t_f)$). If $\varphi(t_f) \in \left(\varphi^{(2)}(t_f), \varphi_{\max}\right]$, then there are no solutions.

For each found pair $\varphi(t_f)$ and β', we calculate ρ (for example, from (5.2)).

Let us express the inclination angle β of the velocity vector of system (2.1) at the instant $t_0 = 0$ relative to the direction of the SSL through its inclination at the instant t_f. We have $\beta = \beta' + \varphi(t_f)$. With this value β, we integrate equation (3.5) from the instant t_f to the instant $t_0 = 0$. As edge conditions at time t_f, we take the values $\varphi = \varphi(t_f)$ and $\dot{\varphi}(t_f) = 0$. We obtain the control $u(t) = \dot{\varphi}(t)$ on the interval $[t_0, t_f]$.

We use the found control in system (2.1) with the initial condition $(x(t_0), y(t_0), \varphi(t_0))^{\mathsf{T}} = (0,0,0)^{\mathsf{T}}$. We find the motion $(x(\cdot), y(\cdot))^{\mathsf{T}}$ and, in particular, its last position $\left(x(t_f), y(t_f)\right)^{\mathsf{T}}$.

Changing $\varphi(t_f)$ from 0 till $\varphi^{(2)}(t_f)$, we obtain the set of endpoints of the motions by virtue of all possible controls $U^{(+)}$. Such a set forms a curve, which we denote by $F^{(+)}$.

3) Consider the motion $(x(\cdot), y(\cdot), \varphi(\cdot))^{\mathsf{T}}$ generated by some control $u(\cdot) \in U^{(-,+)}$. Such a control is of the type U_2. The corresponding reverse control $u^{\#}(t) = u(t_f - t)$, due to symmetry property 2 from Section 3.1, leads to the phase state $\left(x^{\#}(t_f), y^{\#}(t_f), \varphi(t_f)\right)^{\mathsf{T}}$, for which the points $(x,y)^{\mathsf{T}}$ and $\left(x^{\#}, y^{\#}\right)^{\mathsf{T}}$ are mirror symmetric to each other about the axis X. Therefore, instead of studying the motion due to the control $u(\cdot)$, we can take the motion due to the reverse control $u^{\#}(\cdot)$.

The control $u^{\#}(\cdot)$ is of the type U_3. For $u^{\#}(\cdot)$, we obtain the edge condition at the initial time: $u^{\#}(t_0) = 0$. When constructing the motion due to the control $u^{\#}(\cdot)$, we will use formulas (7.6), (7.7) from paper [13]. We have

$$t_f = \frac{1}{\sqrt{2\rho}} \left(\int_0^{\varphi_3} \frac{d\varphi}{\sqrt{\cos\beta' - \cos(\varphi+\beta')}} + \int_0^{\varphi_3+\varphi(t_f)} \frac{d\varphi}{\sqrt{\cos\beta' - \cos(\varphi+\beta')}} \right), \qquad (5.4)$$

$$\mu = \sqrt{2\rho} \left(\int_0^{\varphi_3} \sqrt{\cos\beta' - \cos(\varphi+\beta')}\, d\varphi + \int_0^{\varphi_3+\varphi(t_f)} \sqrt{\cos\beta' - \cos(\varphi+\beta')}\, d\varphi \right). \qquad (5.5)$$

Here β' is the angle counted counterclockwise from the velocity vector direction of system (2.1) at the instant t_1 of the control sign change till the SSL direction. The symbol ρ denotes the constant used in relation (3.5). The symbol φ_3 is the angle taken in absolute value, which is accumulated on the interval $[t_1, t_f]$. The quantities φ_3, $\varphi(t_f)$ and β' are related (see Fig. 11) by the equality

$$2\beta' + \varphi_3 + \varphi(t_f) = 2\pi. \qquad (5.6)$$

3a) Let us explain formula (5.4). A similar explanation applies to (5.5).

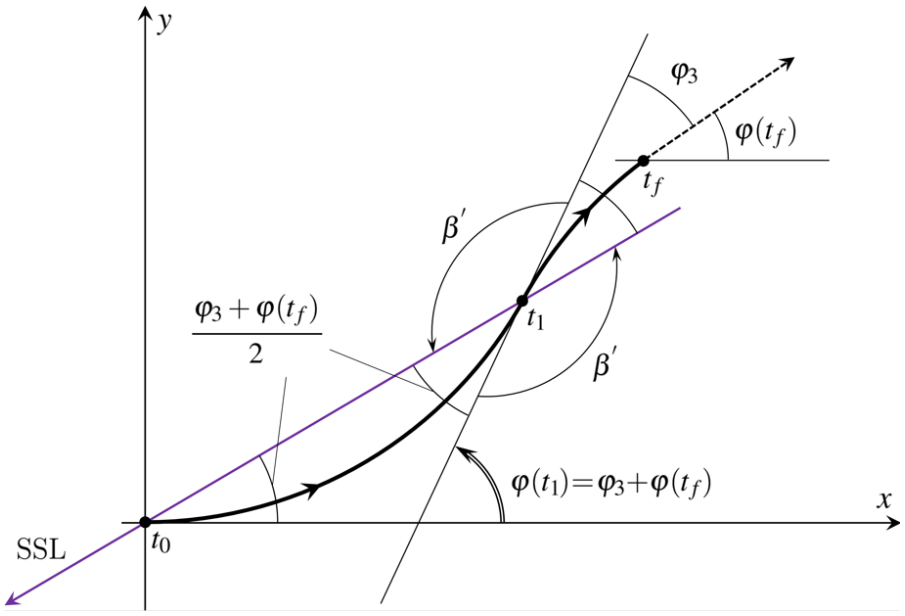

FIGURE 11. Explanation of angles in formula (5.6)

Based on (3.9) and using in formula (3.7) the sign "+" in front of the root, when we consider the first interval, and the sign "−", when we consider the second one, we obtain

$$t_f=(t_1-t_0)+(t_f-t_1)=\int_0^{\varphi_3+\varphi(t_f)}\frac{d\varphi}{\sqrt{c_*-2\rho\cos(\varphi-\beta)}}+\int_{\varphi_3+\varphi(t_f)}^{\varphi(t_f)}\frac{d\varphi}{-\sqrt{c_*-2\rho\cos(\varphi-\beta)}}.$$

In both integrals, we make the substitution $\varphi'=(\varphi_3+\varphi(t_f))-\varphi$. Then $d\varphi'=-d\varphi$. The value $\varphi=0$ corresponds to $\varphi'=\varphi_3+\varphi(t_f)$, the value $\varphi=\varphi_3+\varphi(t_f)$ is replaced by $\varphi'=0$, and the value $\varphi=\varphi(t_f)$ by $\varphi'=\varphi_3$. Introducing the notation $\beta'=\beta-(\varphi_3+\varphi(t_f))$, we obtain

$$\begin{aligned}t_f&=\int_{\varphi_3+\varphi(t_f)}^{0}\frac{-d\varphi'}{\sqrt{c_*-2\rho\cos(-\varphi'-\beta')}}+\int_0^{\varphi_3}\frac{-d\varphi'}{-\sqrt{c_*-2\rho\cos(-\varphi'-\beta')}}\\&=\int_0^{\varphi_3+\varphi(t_f)}\frac{d\varphi'}{\sqrt{c_*-2\rho\cos(\varphi'+\beta')}}+\int_0^{\varphi_3}\frac{d\varphi'}{\sqrt{c_*-2\rho\cos(\varphi'+\beta')}}.\end{aligned}$$

The last expression on the right side coincides with (5.4). The meaning of the angle β' is the same as given in the description of formula (5.4). The symbol φ' is treated as the variable of integration.

3b) We express φ_3 through $\varphi(t_f)$, β' from (5.6) and substitute into (5.4), (5.5). By writing the product $t_f\cdot\mu$, we exclude ρ and obtain a relation connecting the parameters $\varphi(t_f)$ and β'. When numerically solving such an equation for a fixed $\varphi(t_f)\in[0,\varphi^{(1)}(t_f))$, we obtain a single solution (the value of β' depending on $\varphi(t_f)$). If $\varphi(t_f)\geq\varphi^{(1)}(t_f)$, then there are no solutions.

For the found pair $\left(\varphi(t_f),\beta'\right)$, we compute ρ (for example, from (5.5)).

Since $u^{\#}(t)=0$ at the initial instant $t_0=0$ and also at the instant t_1 (in which the control changes sign from "+" to "−"), we can express the angle β of the velocity vector inclination relative to the SSL at the instant t_0 through the angle β' related to the instant t_1. We get $\beta=$

$2\pi-\beta'$. We integrate equation (3.5) for this β from the instant $t_0=0$ to the instant t_f in direct time with initial conditions $\varphi(t_0)=0$ and $\dot\varphi(t_0)=0$. We obtain the control $u^{\#}(t)=\dot\varphi(t)$ on the interval $[t_0,t_f]$.

The required control $u(\cdot)\in U^{(-,+)}$ is found by the formula $u(t)=u^{\#}(t_f-t)$.

Integrating system (2.1) with initial condition $(x(t_0),y(t_0),\varphi(t_0))^{\mathsf T}=(0,0,0)^{\mathsf T}$, we find the motion $x(\cdot)$, $y(\cdot)$ and, in particular, its last position $\big(x(t_f),y(t_f)\big)^{\mathsf T}$.

Changing $\varphi(t_f)$ from 0 till $\varphi^{(1)}(t_f)$, we obtain the set of endpoints of the motions by virtue of all possible controls $U^{(-,+)}$. Such a set forms a curve, which we denote by $F^{(-,+)}$.

4) Consider the case $\varphi(t_f)\in(-\varphi_{\max},0)$. Let us use the constructions for the case $\varphi(t_f)>0$. The controls $U^{(+)}$ and $U^{(-,+)}$ were used there. Now let us take the controls $U^{(-)}$ and $U^{(+,-)}$, which differ only by the change of sign. As a result, we obtain curves $F^{(-)}$ and $F^{(+,-)}$, which are symmetric to the curves $F^{(+)}$ and $F^{(-,+)}$ relative to the axis x.

6. Examples of Numerical Construction of Sets $\mathscr{G}(t_f,\mu)$. Comparison with the Case of Geometric Constraints

For numerical constructions, we assume $\mu=1$.

From what was described in Sections 4 and 5, it follows that the upper part (above the axis x) of the boundary of the set $\mathscr{G}(t_f,\mu)$ is formed by the curves $F^{(+)}$ and $F^{(-,+)}$. The lower part of the boundary is symmetric to the upper part with respect to the axis x (the property 5 in Section 3.1).

1) Let us start with the curves $F^{(+)}$, $F^{(-,+)}$. Figs. 12 – 14 present the result of their numerical construction for $t_f=20$. The curve $F^{(+)}$ consists of two parts marked in light green (the long part) and dark green (the short part). The construction of the curve $F^{(+)}$ is carried out on the basis of the numerical solution of equation (5.3) from the item 2b) of Section 5. The light green part corresponds to the case of unique solution, and the dark green part is the case of two solutions. The curve $F^{(-,+)}$ is marked in red. The description of its construction is set out in the item 3) of Section 5. Additionally, the φ-sections $G_\varphi(t_f,\mu)$ are shown for $\varphi=0.8$ (Fig. 12), $\varphi=2.9$ (Fig. 13), and $\varphi=4.027$ (Fig. 14).

It can be seen that each of the φ-sections shown in Figs. 12 and 13 "hooks" the curve $F^{(+)}$ with one of its boundary points, and the other its point contacts with the curve $F^{(-,+)}$. The boundary of the φ-section $G_\varphi(t_f,\mu)$ presented in Fig. 14 is in contact with the curve $F^{(+)}$ at two points. Here, the boundary of the φ-section between the contact points almost coincides with the curve $F^{(+)}$.

The algorithm from the paper [13] was used to find φ-sections. Theoretically, any φ-section $G_\varphi(t_f,\mu)$ (in our case $\mu=1$, $t_f=20$) is embedded in the set $\mathscr{G}(t_f,\mu)$. This inclusion is used to verify the correctness of the constructions.

Figures 12 – 14 show in yellow color the motions leading to the points of contact of φ-sections with curves $F^{(+)}$ and $F^{(-,+)}$. Each motion finishes on its own SSL (SSL are shown in black). The directions of the SSL are marked with an arrow. The motion in Fig. 12 leading to the point, where the boundary of the φ-section touches the curve $F^{(+)}$, practically goes on the switching line (starting from very small $t>0$). Theoretically, it lies to the left of the SSL without crossing it.

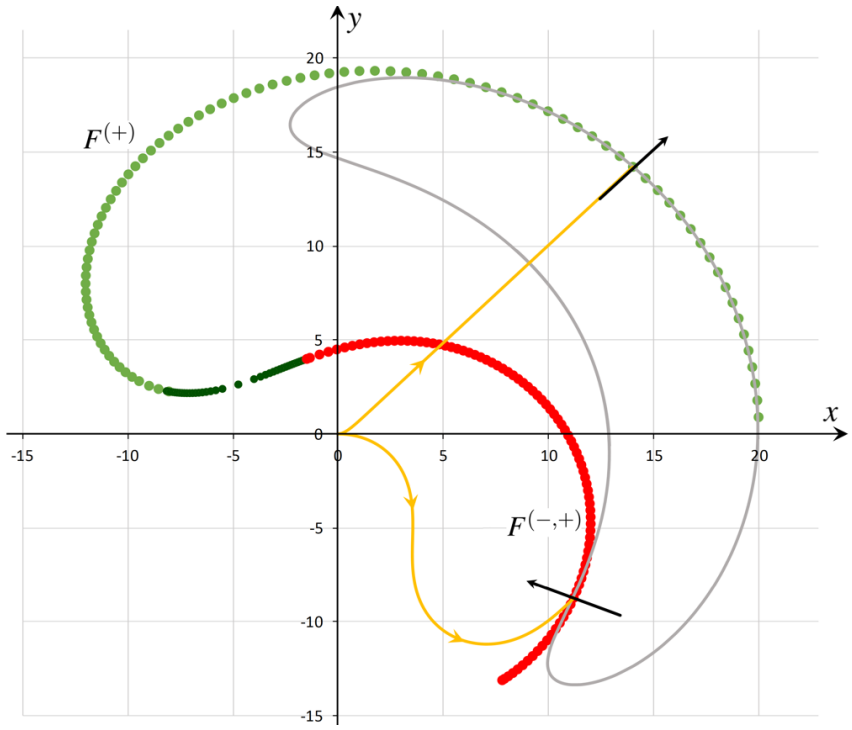

FIGURE 12. The curves $F^{(+)}$, $F^{(-,+)}$ for $t_f = 20, \mu = 1$; the φ-section $G_\varphi(20,1)$ for $\varphi = 0.8$

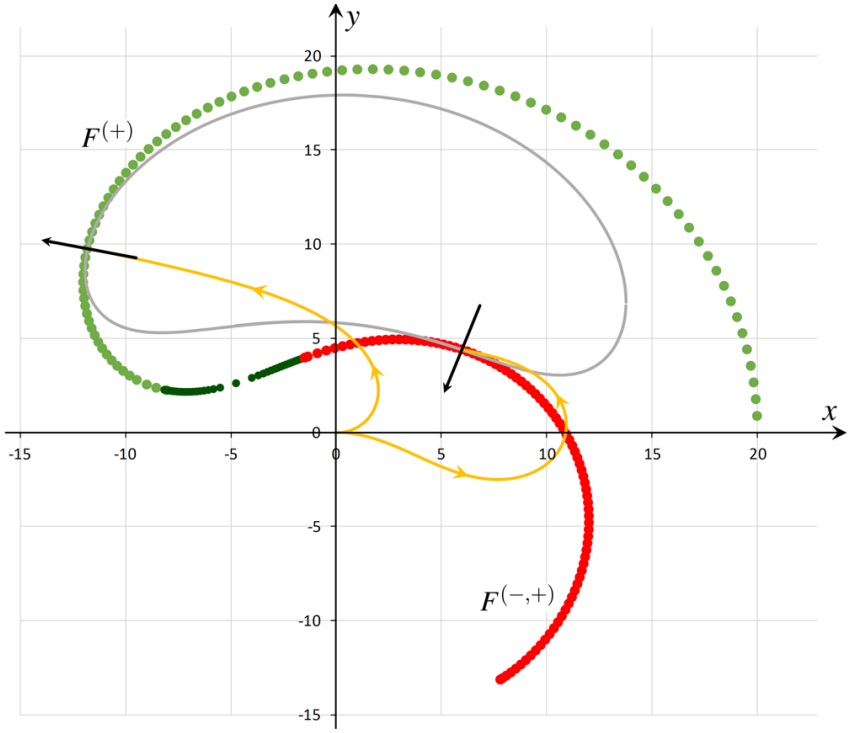

FIGURE 13. The curves $F^{(+)}$, $F^{(-,+)}$ for $t_f = 20, \mu = 1$; the φ-section $G_\varphi(20,1)$ for $\varphi = 2.9$

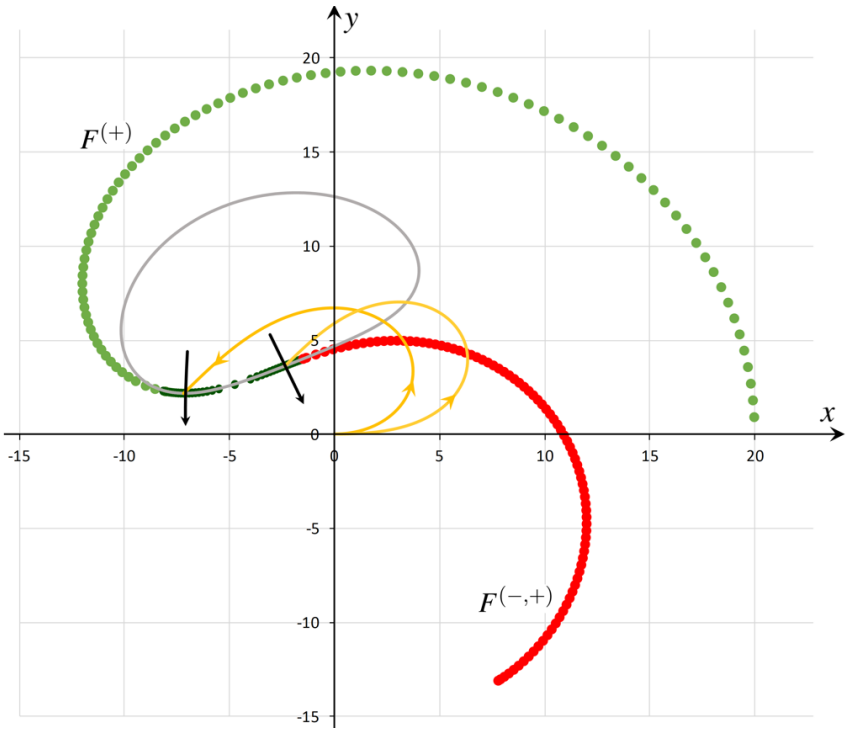

FIGURE 14. The curves $F^{(+)}$, $F^{(-,+)}$ for $t_f = 20, \mu = 1$; the φ-section $G_\varphi(20,1)$ for $\varphi = 4.027$

To construct the boundary of the set $\mathscr{G}(t_f,\mu)$, we take only those parts of the curves $F^{(+)}$ and $F^{(+,-)}$ that are above or on the axis x. This follows from Lemma 4.4.

Fig. 15 additionally explains the construction of the curves $F^{(+)}$ and $F^{(+,-)}$. It shows the numerically calculated graph $\beta' \to \varphi(t_f)$ corresponding to the values $\varphi(t_f)$ and β', which satisfy the product $t_f \cdot \mu$ for $t_f = 20$, $\mu = 1$. Up to the value $\varphi(t_f) = \varphi^{(1)}(t_f) \approx 3.846$, the left root of the equation with respect to β' (the equation is defined by this graph) is used to plot the light green part of the curve $F^{(+)}$, and the right root serves to plot the curve $F^{(-,+)}$. In the range $((\varphi^{(1)}(t_f), \varphi^{(2)}(t_f)] \approx (3.846, 4.058]$, the both roots define points included to the dark green part of the curve $F^{(+)}$. When $\varphi(t_f) \in (\varphi^{(2)}(t_f), \varphi_{\max}(t_f)] \approx (4.058, 4.472]$, there are no solutions. This means that any φ-section of $G_\varphi(t_f,\mu)$ is in the interior of the set $\mathscr{G}(t_f,\mu)$ for $\varphi(t_f) \in (\varphi^{(2)}(t_f), \varphi_{\max}(t_f)]$.

2) For a fixed μ, increasing the value t_f from $t_f = 0$, we find the first value t_f^* when the curve $F^{(+)}$ descends to the axis x to the left of $x = 0$. When $t_f \in (0, t_f^*)$, the set $\mathscr{G}(t_f,\mu)$ is simply connected. Let $t_f^{**} > t_f^*$ be the value t_f closest to t_f^* on the right, at which the curve $F^{(-,+)}$ has only one point on the axis x and all other points lie below the axis x. For $t_f \in [t_f^*, t_f^{**})$, the set $\mathscr{G}(t_f,\mu)$ is not simply connected: there is a "hole" that does not belong to it. The hole degenerates into a point at $t_f = t_f^{**}$.

When $t_f \geq t_f^{**}$, the set $\mathscr{G}(t_f,\mu)$ again becomes simply connected. Its boundary is completely determined by the initial part of the curve $F^{(+)}$ (until its first intersection with the axis x) and the corresponding to it initial part of the curve $F^{(-)}$.

This fact is not obvious. Let us explain it using the symmetry property 4 from Section 3.1. We denote the value μ, that we took, by $\overline{\mu}$. Since the shape of the boundary of the set $\mathscr{G}(t_f,\mu)$

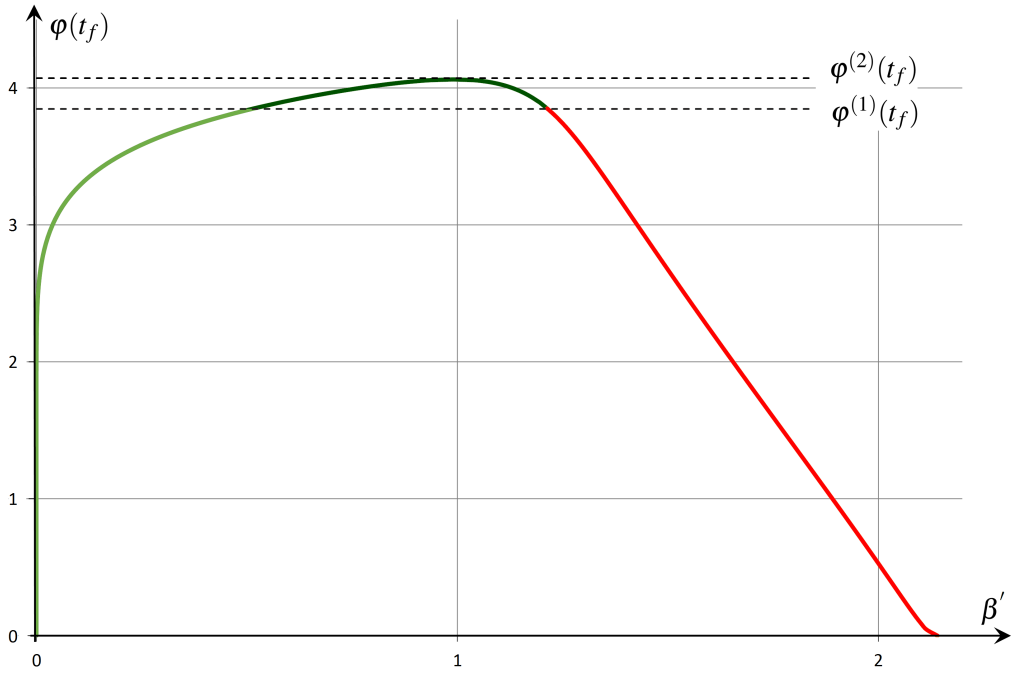

FIGURE 15. Graph of dependence $\varphi(t_f)$ on β' for $t_f = 20$, $\mu = 1$; $\varphi^{(1)}(t_f) \approx 3.846$, $\varphi^{(2)}(t_f) \approx 4.058$

is determined only by the product $t_f \cdot \mu$, then, instead of increasing t_f, we will increase μ starting from $\overline{\mu}$. In this case, we assume that $t_f = t_f^{**}$ is fixed. It is clear that $\mathscr{G}(t_f^{**}, \overline{\mu}) \subset \mathscr{G}(t_f^{**}, \mu)$ for $\mu \geq \overline{\mu}$. Based on it, we establish that the boundary of the set $\mathscr{G}(t_f^{**}, \mu)$ for $\mu \geq \overline{\mu}$ is determined only by the curve $F^{(+)}$ part until the point of its first intersection with the axis x and the corresponding part of the curve $F^{(-)}$, which is symmetric with respect to the axis x.

3) Figure 16 shows the sequence of the sets $\mathscr{G}(t_f, \mu)$ for $\mu = 1$ and six values $t_f = (0.5\pi)^2$, $(\pi)^2, (1.5166\pi)^2$, $(1.6843\pi)^2$, $(1.8166\pi)^2$, $(2\pi)^2$. Each set is depicted in its own scale. The value $t_f = (1.5166\pi)^2$ corresponds to the situation when the curve $F^{(+)}$ touches the axis x from above (correspondingly, the curve $F^{(-)}$ touches the axis x from below). For $t_f = (1.6843\pi)^2$, the junction of the curves $F^{(+)}$ and $F^{(-,+)}$ (respectively, the curves $F^{(-)}$ and $F^{(+,-)}$) occurs at the origin. For $t_f = (1.8166\pi)^2$, the boundary of the "hole" (that does not belong to $\mathscr{G}(t_f, \mu)$) degenerates into a point. As t_f increases further, the set $\mathscr{G}(t_f, \mu)$ is simply connected. Its boundary is completely determined by the parts of the curves $F^{(+)}$ and $F^{(-)}$. The lines shown in Fig. 16 are composed of curves $F^{(+)}$, $F^{(-,+)}$, $F^{(-)}$, $F^{(+,-)}$. Their points satisfy the necessary PMP conditions for motions leading to $\partial\mathscr{G}(t_f, \mu)$ (Theorem 4.1). Then, using Lemmas 4.2, 4.4, and 4.7, some parts of these curves are discarded to obtain the boundary. The required set $\mathscr{G}(t_f, \mu)$ is highlighted in gray.

4) Figure 17 shows the sets $\mathscr{G}(t_f, \mu)$ under the geometric constraint $|u(t)| \leq 1$ for six values $t_f = 0.8\pi, 1.3\pi, 1.814\pi, 2\pi, 2.178\pi, 2.4\pi$, which are chosen so that the structural analogy with the case of the integral constraint can be seen. The fundamental difference in the case of the geometric constraint is the following: if the value of t_f is smaller than the vanishing instant of the hole, then any φ-section $G_\varphi(t_f, \mu)$, $\varphi \in (-\varphi_{\max}, \varphi_{\max}) = (-t_f, t_f)$ is contacted by two points with the boundary of the set $\mathscr{G}(t_f, \mu)$. In this case, one point is on the upper (or lower) curve of

the outer boundary. This curve is the involute. The other point is on the upper (or lower) curve of the inner boundary, which is the cardioid. Thus, under geometric constraint, there is no part on the outer curve, consisting of paired points, each of which contacts with the same φ-section $G_\varphi(t_f,\mu)$ (corresponding to this pair).

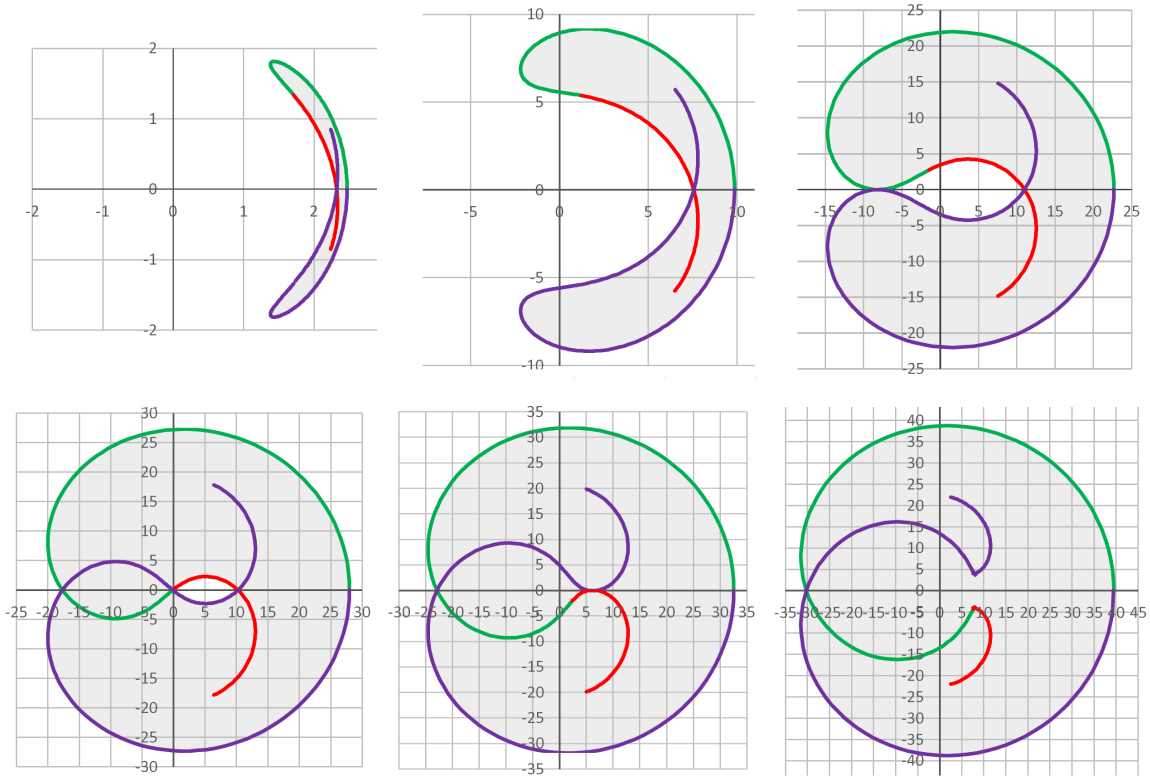

FIGURE 16. Examples of reachable sets $\mathscr{G}(t_f,\mu)$ under the integral control constraint

The points of the curves shown in Fig. 17 satisfy the necessary PMP conditions for the motions leading on $\partial\mathscr{G}(t_f,\mu)$ under the geometric control constraint. After rejecting some parts of these curves (using additional statements from [4] that clarify the necessary conditions), we obtain the set $\mathscr{G}(t_f,\mu)$ highlighted in gray fill.

7. CONCLUSION

The paper is devoted to the theoretical and numerical study of the two-dimensional reachable set "at the instant" for the Dubins car on the plane of the geometric coordinates x,y under the quadratic integral constraint on the scalar control. The study is based on facts obtained earlier for the three-dimensional reachable set in the coordinates x,y,φ, where φ is the inclination angle of the velocity vector.

The structure of the two-dimensional reachable set is well known in the case of the geometric control constraint. In the paper, we analyze the similarity and difference between the structure of the reachable set under the integral control constraint and the reachable set under the geometric constraint.

The work can be useful in solving various optimal control problems for the Dubins car under the integral constraint on control, in particular, in solving time-optimal problems.

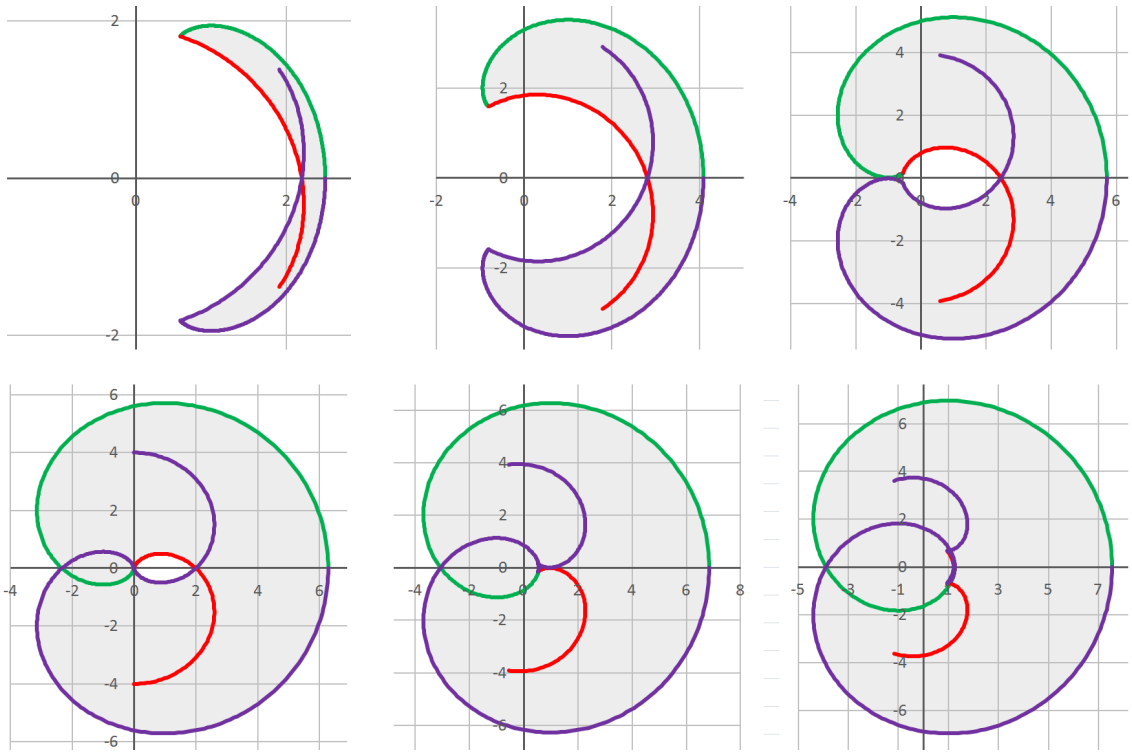

FIGURE 17. Examples of reachable sets $\mathcal{G}(t_f, \mu)$ under the geometric control constraint

Further progress in the study of the two-dimensional reachable set can be associated with an analytical description of its boundary using elliptic functions.

Acknowledgments
The authors are grateful to the reviewer for the very helpful comments.

REFERENCES

[1] V. Shalumov, G. Merkulov, T. Shima, Delayed Decision Guidance in an Integrated Midcourse-Terminal Engagement for Conventional Interceptors, In: 32nd Mediterranean Conference on Control and Automation (MED), pp. 752–757, 2024. doi: 10.1109/MED61351.2024.10566176

[2] M. Buzikov, Computing the Minimum-Time Interception of a Moving Target, J. Optim. Theory Appl. 202 (2024) 975–995.

[3] Y. I. Berdyshev, Synthesis of optimal control for a third-order system, Problems of Analysis of Nonlinear Automatic Control Systems, Sverdlovsk: Inst. Mat. Mekh., UNTs AN USSR, pp. 91–101, 1973. (in Russian).

[4] E. J. Cockayne, G. W. C. Hall, Plane Motion of a Particle Subject to Curvature Constraints, SIAM J. Control Optim. 13 (1975), 197–220.

[5] L. Euler, Methodus inveniendi lineas curvas maximi minimive proprietate gaudentes, sive solutio problematis isoperimitrici latissimo sensu accepti, Geneva, Lausanne, 1744.

[6] R. Levien, The elastica: A mathematical history, Electrical Engineering and Computer Sciences University of California at Berkeley, Technical Report No. UCB/EECS-2008-103, 2008.

[7] A. A. Ardentov, Y.L. Sachkov, Solution to Euler's elastic problem, Automation and Remote Control, 70 (2009), 633–643. doi: 10.1134/S0005117909040092

[8] A. A. Ardentov, Multiple Solutions in Euler's Elastic Problem, Automation and Remote Control, 79 (2018), 1191–1206. doi: 10.1134/S0005117918070020

[9] T. Miura, Polar tangential angles and free elasticae, Mathematics in Engineering, 3 (2021), 1–12, doi: 10.3934/mine.2021034

[10] G. Merkulov, V. Turetsky, T. Shima, Non-Linear-Quadratic Optimal Control Problem for a Unicycle: Maximin Solution, In: 2024 UKACC 14th International Conference on Control (CONTROL), pp. 287–292, 2024. doi: 10.1109/CONTROL60310.2024.10532056

[11] M. I. Gusev, I. V. Zykov, On Extremal Properties of the Boundary Points of Reachable Sets for Control Systems with Integral Constraints, Proceedings of the Steklov Institute of Mathematics, 300 (2018), 114–125. doi: 10.1134/S0081543818020116

[12] V. S. Patsko, G. I. Trubnikov, A. A. Fedotov, Reachable Set of the Dubins Car with an Integral Constraint on Control, Doklady Mathematics, 108 (2023), S34–S41. doi: 10.1134/S106456242360080X

[13] V. S. Patsko, G. I. Trubnikov, A. A. Fedotov, Numerical study of a three-dimensional reachable set for a Dubins car under an integral control constraint, Commun. Optim. Theory, 2025 (2025), 24.

[14] I. V. Zykov, On the Reachability Problem for a Nonlinear Control System with Integral Constraints, CEUR Workshop Proceedings, 1894 (2017), 88–97. (in Russian).

[15] M. I. Zelikin, Theory and applications of the problem of Euler elastica, Russian Mathematical Surveys, 67 (2012), 281–296. doi: 10.1070/RM2012v067n02ABEH004787